Numerical and experimental study of VM type pulse tube cryocooler with multi-bypass operating below 4 K

Changzhao Pan, Jue Wang, Kaiqi Luo, Liubiao Chen, Hai Jin, Wei Cui, Junjie Wang, Yuan Zhou

Numerical and experimental study of VM type pulse tube cryocooler with multi-bypass operating below 4K

Changzhao Pan[1, 2*], Jue Wang[1, 3], Kaiqi Luo[1,3], Liubiao Chen[1], Hai Jin[4], Wei Cui[4], Junjie Wang[1,3] , Yuan Zhou[1,3*]

[1] *Key Laboratory of Cryogenics, Technical Institute of Physics and Chemistry, Chinese Academy of Sciences, Beijing, 100190, China*

[2] *Laboratoire national de métrologie et d'essais-Conservatoire national des arts et métiers (LNE-Cnam), France*

[3] *University of Chinese Academy of Sciences, Beijing, 100049, China*

[4] *Department of Physics and Center for Astrophysics, Tsinghua University, Beijing, 100084, China*

Abstract

The Vuilleumier (VM) type pulse tube cryocooler (VPTC) is a new kind of 4K cryocooler which had been experimentally verified. This paper presents the recent advances on a 4K VPTC in our laboratory. First, the mechanism of multi-bypass was numerically studied using Sage software. The results showed that the function of the multi-bypass is not only similar to a double-inlet, but also to an orifice, which makes the VPTC work like a two-stage cryocooler. Based on the simulation results, the performance of VPTC was experimentally studied. Under its optimal operating conditions, a no-load temperature of 3.7K has been obtained, which is the first demonstration of a single-stage VPTC obtaining temperatures below 4K. It can supply about 14mW cooling power at 4.2K and about 100mW cooling power at 35K simultaneously, which has potential application as the pre-cooler for an adiabatic demagnetization refrigerator (ADR). Finally, based on this VPTC, a new mK cooling chain for HUBS (Hot Universe Baryon Surveyor) satellite is proposed and its prospect has also been theoretically analyzed.

Keywords: VM, thermal-compressor, pulse tube, multi-bypass, 4K cooling chain

*Corresponding author. Tel.:+86 10 82543759; fax: +86 10 62564050.
E-mail addresses:
changzhao.pan@lecnam.com (Changzhao Pan); zhouyuan@ mail.ipc.ac.cn (Yuan Zhou)

1. Introduction

With recent developments in quantum physics and cryoelectronics, the need for cryocooler operating below 4K is increasing. Even though traditional commercial 4K cryocoolers (GM or GM type pulse tube cryocooler) can meet most requirements, the use of advanced detectors, such as superconducting nanowire single-photon detectors (SNSPD)[1], superconducting transition-edge sensor (TES)[2], low-TC SQUIDs[3] and et al., has given rise to some new challenges for its cooling system. Especially in space applications, the cryocooler must have smaller size, lower power consumption, higher efficiency and lower temperature. Therefore, it is important to develop the next generation cryocooler to meet those challenges.

For the traditional 4K cryocooler, some researchers have made efforts on the low-power consumption GM type cryocooler, but the large bulk and high power (~ 1kW[4][5]) is still the main obstacle for its application in space applications. The Joule-Thomson (J-T) cryocooler is the traditional 4 K cryocooler, which has been used in the ASTRO-H [6] and SNSPD missions. This type of cryocooler needs to be precooled by another 20K cryocooler. So this hybrid 4K cooling system has the disadvantage of complexity and some technical risks of internal wear, outgassing, etc. Even worse, some impurities in helium may block the J-T valve and result in cooling system failure[7]. Therefore, it is advantageous to develop alternative cooling methods.

The Multi-stage High frequency Stirling type pulse tube cryocooler (HSPTC) is one relatively new cryocooler capable of reach 4K[8][9][10][11]. Because there are no moving components in its cold finger, the HSPTC has the advantages of compactness,

long life, and low vibration. And based on the Stirling cycle, this type cryocooler should have more potential to obtain a higher efficiency. But until now, HSPTC is very difficult to obtain the temperature below 4K, even by using helium-3[12][13]. That is because HSPTC is normally working at the frequency above 20Hz driven by a linear compressor. The high-frequency oscillating flow generates high pressure drop loss in regenerator, which makes it difficult to achieve high efficiency at 4 K. So a feasible way to increase its efficiency is to develop the Low frequency Stirling type pulse tube cryocooler (LSPTC).

A VM type pulse tube cryocooler (VPTC) is driven by a thermal-compressor, and is a new type of LSPTC. Dai et al. introduced the concept of VPTC and built a cryocooler, which obtained the lowest temperature of 3.5 K by using 77 K and 20 K pre-coolers[14]. This work demonstrated its capacity to operate at liquid helium temperatures. More recently, Wang et al.[15][16] developed a 15 K single-stage VPTC by using an 80 K Stirling type PTC as pre-cooler, and then a lowest temperature of 7.58K has been obtained after optimizing. In our laboratory, VM type cryocooler has been in development for many years. The “first generation” VPTC in our laboratory obtained a no-load temperature of 2.5K [17][18][19]. In our “second generation” VPTC, we removed its displacer in the first stage and developed a single-stage structure for practical application. We successfully obtained a no-load temperature of 4.9K in the second generation VPTC [20]. These results showed great potential to be the next-generation pulse tube cryocooler.

This paper presents the recent advance on the second generation VPTC. First, the

evolution of our VPTC will be presented and its advantages will be discussed. Then, the mechanism of multi-bypass is numerically studied and clarified. After optimizing its performance, the phase relationship distributions and exergy-loss distributions will be presented. The interaction of multi-bypass and double-inlet was studied comprehensively and optimized by experiment. The influence of orifice, operating frequency and average pressure on the multi-bypass was also experimentally studied. Finally, the optimal performance of this VPTC is presented. And based on this VPTC, an alternative sub-kelvin cooling chain is proposed.

2. Evolution of cryogen-free VM type pulse tube cryocooler

Figure 1 shows the evolution from the first generation VPTC to the second generation VPTC and the next-generation VPTC. There are mainly three changes at present work from the first generation:

(1) Cryogen-free. A dry 77K mechanical cryocooler, GM cryocooler (only the first-stage being used), was used to replace the liquid nitrogen as pre-cooler. The facilitated measuring the power consumption of the thermal-compressor. Because the pre-cooling power is used more efficiency, the new structure also increase the efficiency of our second generation VPTC (the exergy efficiency is about 0.6% in our previous paper [18][19], and the exergy efficiency increases to about 0.9% as shown in the next section).

(2) Removed the displacer and reduced the stroke of the thermal-compressor. A pulse tube was used to replace the displacer in the former VPTC. So the vibration would be lower and the heat losses caused by movement were eliminated, such as

the shuttle loss, leakage loss, abrasion loss, etc. In addition, the stroke of thermal-compressor was reduced from 32mm to 20mm, so the input power of our second generation VPTC was much smaller than before. Reducing the stroke was also expected to reduce vibration.

(3) Single-stage structure. A multi-bypass was used to simplify the former gas-coupled structure (two-stage). It makes the system more compact and easier to integrate with applications. The smaller mass is also very important for space applications.

In the next-generation VPTC, a high-efficiency 77K pulse tube cryocooler, currently being designed, will replace the present GM cryocooler. This is a critical step for demonstrating, a hybrid 4K cooling chain that can be used in space.

3. Numerical simulation and discussion

3.1 Ssimulation model

The numerical simulation was conducted by using SAGE10.0 software [21], a 1D simulation program based on Navier-Stokes equations. The LTcooler module was used to build the simulation model of the VPTC. As shown in Figure 2, the whole model was composed by each submodule, and the parameters of each part are shown in table 1. In the simulation, the operating frequency was kept at 2Hz, and the average pressure at 1.0MPa. In order to analyze the mechanism of multi-bypass and its difference from a double-inlet, the resistance of orifice (capillary tube) was set a constant value.

3.2 Simulation results and discussions

3.2.1 The mechanism of multi-bypass

Multi-bypass, invented by Zhou and Han, enables the PTC to reach a lower temperature [22]. By using a multi-bypass, a single-stage SPTC has obtained a no-load temperature of 13.9K, which was better than some two-stage SPTC[23][24]. In our previous work, the multi-bypass was used in the VPTC and obtained a lowest temperature of 4.9K [20]. To further clarify its mechanism, its function was numerically compared with double-inlet, because double-inlet has been studied widely.

Figure 3 (a-d) shows the simulation results. Figure 3-a and 3-b are the results of double-inlet and figure 3-c and 3-d are the results of multi-bypass. Similar to the double-inlet, there exists an optimal value for the opening of the multi-bypass that yields the lowest no-load temperature. Different from the double-inlet, the temperature of multi-bypass stage would decrease with the opening of multi-bypass because some amount of working gas would flow through multi-bypass and generate cooling effect. But for the double-inlet, the temperature of multi-bypass stage (the same position) would increase. It is because the double-inlet would decrease the input acoustic power of cryocooler.

Similar to the double-inlet, the multi-bypass can improve the phase relationship between mass flow rate and pressure in the cold end, shown in the figure 3-d. But the phase adjusting capability of multi-bypass is weaker than double-inlet. On the other hand, the optimal opening of multi-bypass for the lowest temperature does not correspond to the best phase relationship. It is different from double-inlet in which the optimal opening was the same for the lowest temperature and phase relationship. It

147 can be explained from the viewpoint of input acoustic power. With the opening of
148 multi-bypass or double-inlet, the input acoustic power of regenerator-2 would
149 decrease correspondingly. But the input acoustic power of regenerator-2 decreased
150 more obvious with increasing of multi-bypass. So before its phase relationship
151 reaching to the optimal value, the input acoustic power has decreased too small to
152 generate enough cooling power to overcome heat losses, which makes it higher
153 temperature at the optimal phase relationship.

154 **3.2.2 The interaction between double-inlet and multi-bypass**

155 Figure 4 shows the interaction between a double-inlet and multi-bypass. The
156 opening of the multi-bypass has values of 0.3mm, 0.4mm and 0.5mm, but the opening
157 of double-inlet varied from 0.3-0.9mm. When a multi-bypass is used, the double-inlet
158 has two effects. First, the temperature of the multi-bypass stage decreases with the
159 increasing opening of double-inlet, which is different from the trend in Figure 3-a.
160 This further showed that multi-bypass has a cooling effect similar to another stage.
161 Second, the optimal opening of the double-inlet depends on the opening of the
162 multi-bypass. The optimal value first decreases and then increase, and after the best
163 coupling with multi-bypass, its optimal value would decrease slightly. Based on this
164 optimization process, a lowest temperature of 3.69K was obtained with the optimal
165 opening of multi-bypass 0.4mm and double-inlet 0.8mm. With these parameters, the
166 temperature of multi-bypass stage was about 34.8K.

167 **3.2.3 The distribution of phase relationship**

168 The distributions of phase relationship in the VPTC are presented in Figure 5.

169 Here, the phase angles were expressed by the leading angle of mass flow rate to
170 pressure. Because the phase of pressure almost didn't change in the VPTC, the
171 positive real axis was used to present all the phases of pressure. In figure 5, if the
172 mass flow rate is in quadrant I or II, it meant the mass flow rate leaded the pressure.
173 But if the mass flow rate is in quadrant III or IV, it meant the mass flow rate lagged
174 pressure. Here, the subscript "tc" means thermal-compressor, the subscript "r" means
175 regenerator, the subscript "p" means pulse tube, the subscript "i" means inlet, and the
176 subscript "o" means outlet. The subscript "1" and "2" can be found in figure 1.

177 In figure 5, the red arrows located at the III quadrant are the phase relationships
178 in the thermal-compressor. This means the propagation direction of acoustic power
179 was negative. Therefore, in the VPTC, the acoustic power is generated in the cold
180 cavity of thermal-compressor and propagated into the pulse tube cryocooler and the
181 hot end of thermal-compressor. Figure 5-a shows the distributions of phase
182 relationship without double-inlet and multi-bypass. It is the typical phase relationship
183 in the orifice type pulse tube cryocooler [25]. Figure 5-b shows the distributions of
184 phase relationship at the optimal condition. Even though the phase of mass flow rate
185 was still leading the pressure in the regenerator, the phase difference has been reduced,
186 as seen in the phase of $\dot{m}_{r2,o}$. This result was also shown in figure 3. The main reason
187 was the phase in the pulse tube had been changed by the double-inlet and
188 multi-bypass. As shown in figure 5-b, because of the effect of multi-bypass, the phase
189 of mass flow rate was almost same as the pressure at the outlet of pulse tube 2. This
190 relationship is the same as for an orifice pulse tube cryocooler. So from the view of

phase relationship, the multi-bypass has functions like an orifice, yielding behavior similar to a two-stage cryocooler. And for the double-inlet, figure 5-b shows that it would make the phase of mass flow rate lag to the pressure at the outlet of pulse tube 1. So it would realize the same-phase for the mass flow rate and pressure in the midpoint of pulse tube 1. This also reduces the phase difference at the cold end.

In sum, the simulation showed the multi-bypass has two functions. First, multi-bypass has the similar function as double-inlet (located at lower temperature), which can improve the phase relationship in the cold end and reduce acoustic power transferring to the cold end. Second, multi-bypass has the similar function as orifice, which makes it work like as another stage, generating a lower temperature at the position of the multi-bypass.

3.2.4 The distribution of exergy loss

Finally, figure 6 shows the distribution of exergy loss in VPTC. Here, we refer the reader to our previous work [18] for the detailed definition of exergy loss. As mentioned previously, the acoustic generated in the cold cavity of thermal-compressor. The acoustic power, as exergy flow, flows into thermal-compressor and cryocooler. In the optimal case, a total of 23.25W acoustic power is generated in the cold cavity of the thermal-compressor. About 8.5W of acoustic power flowed into the thermal-compressor, and about 14.75W of acoustic power flowed into the cryocooler. Figure 6 also gives the amount and the percentage of exergy loss in each part. The results shows that the main exergy loss in the thermal-compressor was the loss in the heat exchanger, and the main exergy loss in the cryocooler was the loss in the

213 regenerator. There is additional exergy loss in the thermal-compressor, the shuttle loss
214 caused by movement of the displacer. Its value was about 20W, so it is the largest loss
215 in the VPTC. For this case, a total of about 43.25W cooling-power is needed to
216 precool the VPTC at 77K.

217 **4. Experiment and discussions**

218 **4.1 Experimental system**

219 Figure 7 shows the picture of the experimental system. It was the same as our
220 previous system [20], and was precooled by Sumitomo RDK-415D cryocooler. As
221 shown in the figure 7, the displacer of thermal-compressor was driven by a crankshaft.
222 Its stroke was about 20mm, and operated at the range 0~3Hz. The pulse tube
223 cryocooler was coaxial in structure and a picture of each part can be found in figure 7.
224 The detailed parameters of thermal-compressor and pulse tube cryocooler can be
225 found in table 1. In the experiment, the pressure in the hot cavity was measured by a
226 capacitive differential pressure sensor. The temperature was measured by Rh–Fe
227 resistance thermometer calibrated by TIPC (with accuracy of 0.1 K).

228 **4. 2Experimental results and discussions**

229 **4. 2.1 Interaction between double-inlet and multi-bypass**

230 In order to find the optimal interaction between double-inlet and multi-bypass,
231 three multi-bypasses with different opening of double-inlet were studied: 0.38mm,
232 0.5mm and 0.55mm. The case of 0.45mm multi-bypass has been studied in our
233 previous work [20], but the influence of double-inlet was not studied in that case, so it
234 was not used to compare with the other results. Figure 8 shows the influence of

double-inlet on the different openings of the multi-bypass. The optimal double-inlet for the multi-bypass of 0.38mm was about 0.75mm. For the multi-bypass of 0.5mm, its optimal value decreased to about 0.6mm, and then increases to about 0.75mm for the multi-bypass of 0.55mm. Its changing trend was partly consistent with the simulation results in the figure 4. In the simulation, the optimal opening of double-inlet would decrease again after the best coupling value, but the optimal value in the experiment did not follow that trend. This discrepancy has been found in other reference by using Sage software [18] [26]. This is mainly because that Sage is a 1-D software, which cannot simulate the flow and heat transfer in the cryocooler accurately, especially in such low temperature.

In the present experimental results, the optimal opening of multi-bypass was about 0.5mm and the corresponding opening of double-inlet was about 0.65mm. With this optimal opening, this VPTC has obtained a lowest no-load temperature of 3.7K, and it can supply about 14mW cooling power at 4.2K. It is the first time for single-stage VPTC to obtain the temperature below 4K. Its performance has reached or even exceeded some two-stage VPTC [14].

4.2.2 Influence of orifice

The orifice, as the traditional phase shifting method, has an important effect on the operating parameters of a VPTC. As shown in our previous work, a capillary tube was used as the orifice. In present work, a length of 50mm capillary tube was added on the former capillary tube (∅1mm × 3m), called capillary tube-1. The influence of its inner diameter was studied in the present experiment.

Figure 9 shows the influence of capillary tube-1 on the temperature of cold end and multi-bypass stage. With an increase of the inner diameter of capillary tube-1, the temperature of cold end would decrease. But for the temperature of multi-bypass stage, its temperature would increase first and then decrease. It is to say that a higher or lower resistance of orifice all can obtain a lower temperature for the multi-bypass. The reason is related to its optimal operating frequency, as shown in the figure 10.

Figure 10 shows that the optimal operating frequency was in positive correlation with the diameter of capillary tube. A higher operating frequency would consume more pre-cooling power in the thermal-compressor and result in a higher inlet temperature of hot end. That is because a lower resistance of orifice means more working gas flowing into pulse tube and gas reservoir. Also, a higher phase shifting capacity is needed to satisfy the phase relationship in the PTC. So its optimal operating frequency would increase to improve its phase adjusting capability. On the other hand, the temperature of multi-bypass stage is affected by both the amount of working gas and the inlet temperature of hot end. A lower orifice resistance can also lead more working gas flowing through the multi-bypass and generate a more significantly cooling effect, which can make a lower temperature of multi-bypass stage. On the contrary, it would lead a higher inlet temperature of hot end, which can make a higher temperature of multi-bypass stage. Therefore, the lower inlet temperature of hot end makes a lower temperature of multi-bypass stage for capillary tube of 0.5mm, and a more amount of working gas flowing through the multi-bypass also makes a lower temperature of multi-bypass stage for capillary tube of 0.7mm and

279 1mm.

280 **4.2.3 Influence of operating parameters**

281 Figure 11 shows the influence of operating frequency on the temperature of
282 multi-bypass stage and cold end. There is an optimal operating frequency (about
283 1.57Hz) for the cold end. But for the multi-bypass, its temperature would increase
284 with an increase of operating frequency. This is mainly because a higher operating
285 frequency generates a larger flowing resistance, which results in a smaller amount of
286 working gas flowing through multi-bypass stage. Besides, the inlet temperature of hot
287 end would increase with the increasing of operating frequency. Those all result in a
288 higher temperature of the multi-bypass stage.

289 Figure 12 shows the influence of average pressure on the temperature of
290 multi-bypass stage and cold end. Similar to the influence of operating frequency, there
291 is an optimal average pressure (about 1.2MPa) for the temperature of cold end. But
292 for the multi-bypass, its temperature would increase with the increase of average
293 pressure. The main reason is that a higher average pressure increases the loading of
294 the regenerator and the inlet temperature of hot end. Those all make the temperature
295 of multi-bypass stage higher.

296 **4.2.4 Thermal performance**

297 After optimizing all above parameters, a lowest no-load temperature of 3.7K has
298 been obtained in present VPTC, and a corresponding temperature of multi-bypass
299 stage of about 33.2K. Figure 13 and figure 14 show the cooling power of the cold end
300 and multi-bypass. The cold end can supply about 14mW cooling power at the

temperature of 4.2 K, and its multi-bypass can supply above 100mW cooling power at the temperature of 35K. In this condition, the pre-cooling temperature of the GM cryocooler was about 45K and the temperature of hot end (VPTC) was about 80K. When 100mW heating was added at the multi-bypass stage, the temperature of cold end increased just 0.08K. So this VPTC can supply cooling power at cold end and multi-bypass stage simultaneously. Because this VPTC needs only about 35W precooling power at 80K, its total input electrical power of this cryocooler should be below 400W when a high-efficiency 77 K PTC is used as pre-cooler. So the relative Carnot efficiency of present VPTC could reach higher than 0.25%.

5. Prospect of its application in cooling system of HUBS

HUBS (Hot Universe Baryon Surveyor) is being conceptualized in China as a major X-ray mission for the next decade. It is designed to be highly focused scientifically, with the primary driver being to look for "missing baryons". The superconducting transition-edge sensor (TES) is the key technology in HUBS, which requires cooling to below 100mK.

Based on this VPTC, a new cooling chain from 300K to 100mK can be designed, as shown in figure 15. This cooling chain can supply cooling to three radiation shields at 80K, 35K and 3.7K respectively. Considering the areas of each radiation shield (0.9 m^2, 0.5 m^2 and 0.2 m^2), the theoretical radiation load for each is about 7.5W@80K, 15mW@35K and 0.25mW@4K respectively. Adding the heat consumption for the thermal-compressor, this cooling chain needs no more than 45W cooling power at 77K. By using two 25W@77K high-efficiency PTC as pre-cooler on the both sides of

thermal-compressor, the total input electrical power could be below 600W. So it is theoretically possible that this new cooling chain has the capability of pre-cooling the ADR and isolating radiation heat leakage for ADR. In the future works, the VPTC with two multi-bypasses or two-stage VPTC may be designed and built to obtain the temperature around 2.2K. In that case, a single-stage ADR could obtain the temperature below 100mK.

6. Conclusion

In this paper, the recent advance on the 4K VPTC in our laboratory is presented. The most important element of the VPTC, the multi-bypass, was numerically studied. From the view of phase relationship and acoustic power of cold end, the function of the multi-bypass is similar to a double-inlet, and from the view of the distribution of phase difference, its function is similar to an orifice. Those two aspects make it work effectively as a two-stage cryocooler.

The factors that impact the performance of VPTC were experimentally studied. The results showed that the best coupling of multi-bypass and double-inlet for this VPTC is 0.5mm opening of multi-bypass and 0.65mm opening of double-inlet. For the orifice, it can change the optimal operating frequency of VPTC, and then affect the lowest temperature of cold end. For the operating parameters, the results showed that a higher operating frequency and a higher average pressure can result a higher temperature on the multi-bypass stage. But for the temperature of cold end, there existed an optimal value for each factor, which were 1.57Hz for frequency and 1.2MPa for average pressure. Finally, after optimization, a no-load temperature of

3.7K has been obtained in this VPTC, and it can supply about 14mW cooling power and about 100mW cooling power at 35K simultaneously,

Based on this VPTC, a new cooling chain from 300K to 100mK is proposed. After further development, the GM precooler in present system will be replaced by another 77K HSPTC, a key step in demonstrating a spaceworty cooling system for the HUBS satellite.

Acknowledges

This work was supported by the Postdoctoral Innovation Talent Support Program of China (Foundation No. BX201600173). Strategic Pilot Projects in Space Science of China (Foundation No. XDA15010400).

References

[1] Marsili F, Verma V B, Stern J A, et al. Detecting single infrared photons with 93% system efficiency[J]. Nature Photonics, 2013, 7(3): 210.

[2] Miller N A, O'Neil G C, Beall J A, et al. High resolution x-ray transition-edge sensor cooled by tunnel junction refrigerators [J]. Applied Physics Letters, 2008, 92(16): 163501.

[3] Schmidt B, Falter J, Schirmeisen A, et al. A SQUID system for geophysical measurements cooled by a pulse tube cryocooler [J]. Superconductor Science and Technology, 2018, 31(7): 075006.

[4] Hiratsuka Y, Bao Q, Xu M Y. Performance estimation of an oil-free linear compressor unit for a new compact 2K Gifford-McMahon cryocooler[C]//IOP

Conference Series: Materials Science and Engineering. IOP Publishing, 2017, 278(1): 012050.

[5] Schmidt B, Vorholzer M, Dietrich M, et al. A small two-stage pulse tube cryocooler operating at liquid Helium temperatures with an input power of 1 kW [J]. Cryogenics, 2017, 88: 129-131.

[6] Kanao K, Yoshida S, Miyaoka M, et al. Cryogen free cooling of ASTRO-H SXS Helium Dewar from 300 K to 4 K[J]. Cryogenics, 2017, 88: 143-146.

[7] Sato Y, Shinozaki K, Sawada K, et al. Outgas analysis of mechanical cryocoolers for long lifetime[J]. Cryogenics, 2017, 88: 70-77.

[8] Nast T, Olson J, Champagne P, et al. Development of a 4.5 K pulse tube cryocooler for superconducting electronics. In: Advances in cryogenic engineering: transactions of the cryogenic engineering conference-CEC, vol. 53. AIP Publishing; 2008, 985(1).p. 881–6.

[9] Zhi XQ, Han L, Dietrich M, et al. A three-stage Stirling pulse tube cryocooler reached 4.26 K with He-4 working fluid. Cryogenics 2013; 58:93–6.

[10] Quan J, Liu Y, Liu D, et al. 4 K high frequency pulse tube cryocooler used for terahertz space application. Chin Sci Bull 2014; 59(27):3490–4.

[11] Liubiao C, Xianlin W, Xuming L, et al. Numerical and experimental study on the characteristics of 4 K gas-coupled Stirling-type pulse tube cryocooler J]. International Journal of Refrigeration, 2018, 88: 204-210.

[12] Dotsenko V V, Delmas J, Webber R J, et al. Integration of a 4-Stage 4 K pulse tube cryocooler prototype with a superconducting integrated circuit [J]. IEEE

Transactions on Applied Superconductivity, 2009, 19(3): 1003-1007.

[13] de Waele A. Cryocoolers near their low-temperature limit [J]. Cryogenics, 2015, 69: 18-25.

[14] Dai W, Matsubara Y, Kobayashi H. Experimental results on VM type pulse tube refrigerator [J]. Cryogenics, 2002, 42(6): 433-437.

[15] Wang Y, Zhao Y, Zhang Y, et al. Advances on a cryogen-free Vuilleumier type pulse tube cryocooler [J]. Cryogenics, 2017, 82: 62-67.

[16] Wang Y, Wang X, Dai W, et al. A cryogen-free Vuilleumier type pulse tube cryocooler operating below 10 K [J]. Cryogenics, 2018, 90: 1-6.

[17] Pan C, Zhang T, Zhou Y, et al. A novel coupled VM-PT cryocooler operating at liquid helium temperature. Cryogenics 2016:20–4.

[18] Zhang T, Pan C, Zhou Y, et al. Numerical investigation and experimental development on VM-PT cryocooler operating below 4 K. Cryogenics 2016;80:138–46.

[19] Wang J, Pan C, Zhang T, et al. A novel method to hit the limit temperature of Stirling-type cryocooler [J]. Journal of Applied Physics, 2018, 123(6): 063901.

[20] Pan C, Wang J, Luo K, et al. Progress on a novel VM-type pulse tube cryocooler for 4 K[J]. Cryogenics, 2017, 88: 66-69.

[21] Gedeon D. Sage user's guide. Sage v10 ed. Gedeon Associates; 2014.

[22] Zhou Y, Han YJ. Pulse tube refrigerator research. In: 7th International cryocooler conference proceedings 1993; p. 147–50.

[23] Chen L, Jin H, Wang J, et al. 18.6 K single-stage high frequency multi-bypass

411 coaxial pulse tube cryocooler [J]. Cryogenics, 2013, 54: 54-58.
412 [24] Zhou Q, Chen L, Zhu X, et al. Development of a high-frequency coaxial
413 multi-bypass pulse tube refrigerator below 14K[J]. Cryogenics, 2015, 67: 28-30.
414 [25] Radebaugh R, Lewis M, Luo E, et al. Inertance tube optimization for pulse tube
415 refrigerators[C]//AIP Conference Proceedings. AIP, 2006, 823(1): 59-67.
416 [26] Xu J, Zhang L, Hu J, et al. An efficient looped multiple-stage
417 thermoacoustically-driven cryocooler for liquefaction and recondensation of
418 natural gas [J]. Energy, 2016, 101: 427-433.
419

Figure Captions:

Table 1 System configuration parameters

	Components	Parameters
Thermal-compressor	Hot heat exchanger	Diameter of 5 mm, length of 200 mm
	Regenerator	Annular structure, inner diameter of 23.6 mm, outer diameter of 45 mm, length of 120 mm, filling 80# stainless steel screens (SS) with porosity of 70.7 %
	Cold heat exchanger	Diameter of 3 mm, length of 200 mm
PTC	Regenerator 1-1	Annular structure, inner diameter of 12.5 mm, outer diameter of 30 mm, length of 40 mm, filling 200# stainless steel screens (SS) with porosity of 69.1 %
	Regenerator 1-2	Annular structure, inner diameter of 12.5 mm, outer diameter of 30 mm, length of 50 mm, filling lead sphere (0.4mm), with porosity of 37 %
	Regenerator 2-1	Annular structure, inner diameter of 8.5 mm, outer diameter of 18 mm, length of 40 mm, filling Er_3Ni sphere (0.2mm), with porosity of 37 %
	Regenerator 2-2	Annular structure, inner diameter of 8.5 mm, outer diameter of 18 mm, length of 40 mm, filling $HoCu_2$ sphere (0.2mm), with porosity of 37 %
	Pulse tube 1	Diameter of 12.1 mm, length of 90 mm
	Pulse tube 2	Diameter of 8.5 mm, length of 80 mm
Phase shifters	Capillary tube & Reservoir	Diameter of 1 mm, length of 2500 mm Volume of gas reservoir is 5×10^{-4} m^3
	Double-inlet	Opening from 0~0.5mm
	Multi-bypass	Opening from 0~1mm (×4)

Figure 1 The evolution from hybrid two-stage gas-coupled VPTC to the single-stage VPTC with multi-bypass.

Figure 2 The simulation model in the Sage software.

Figure 3 Simulation results of the interaction between double-inlet and multi-bypass.

Figure 4 The distributions of phase difference in the VPTC. (a. without multi-bypass and double-inlet; b. with optimal multi-bypass and double-inlet)

Figure 5 The distributions of exergy loss in the VPTC.

Figure 6 The picture of experimental system.

Figure.7 The simulation results of double-inlet and multi-bypass (a. the temperatures changing with different double-inlet; b. the phase differences with different double-inlet; c. the temperatures changing with different multi-bypass; d. the phase differences with different multi-bypass).

Figure.8 The interaction between double-inlet and multi-bypass.

Figure.9 The influence of orifice on the temperature of cold end and multi-bypass.

Figure.10 The influence of orifice on the optimal operating frequency and inlet temperature of hot end.

Figure.11 The influence of operating frequency on the temperature of cold end and multi-bypass.

Figure.12 The influence of average pressure on the temperature of cold end and multi-bypass.

Figure.13 The cooling power of cold end.

Figure.14 The cooling power of multi-bypass.

Figure.15 The design of new mK cooling chain for HUBS.

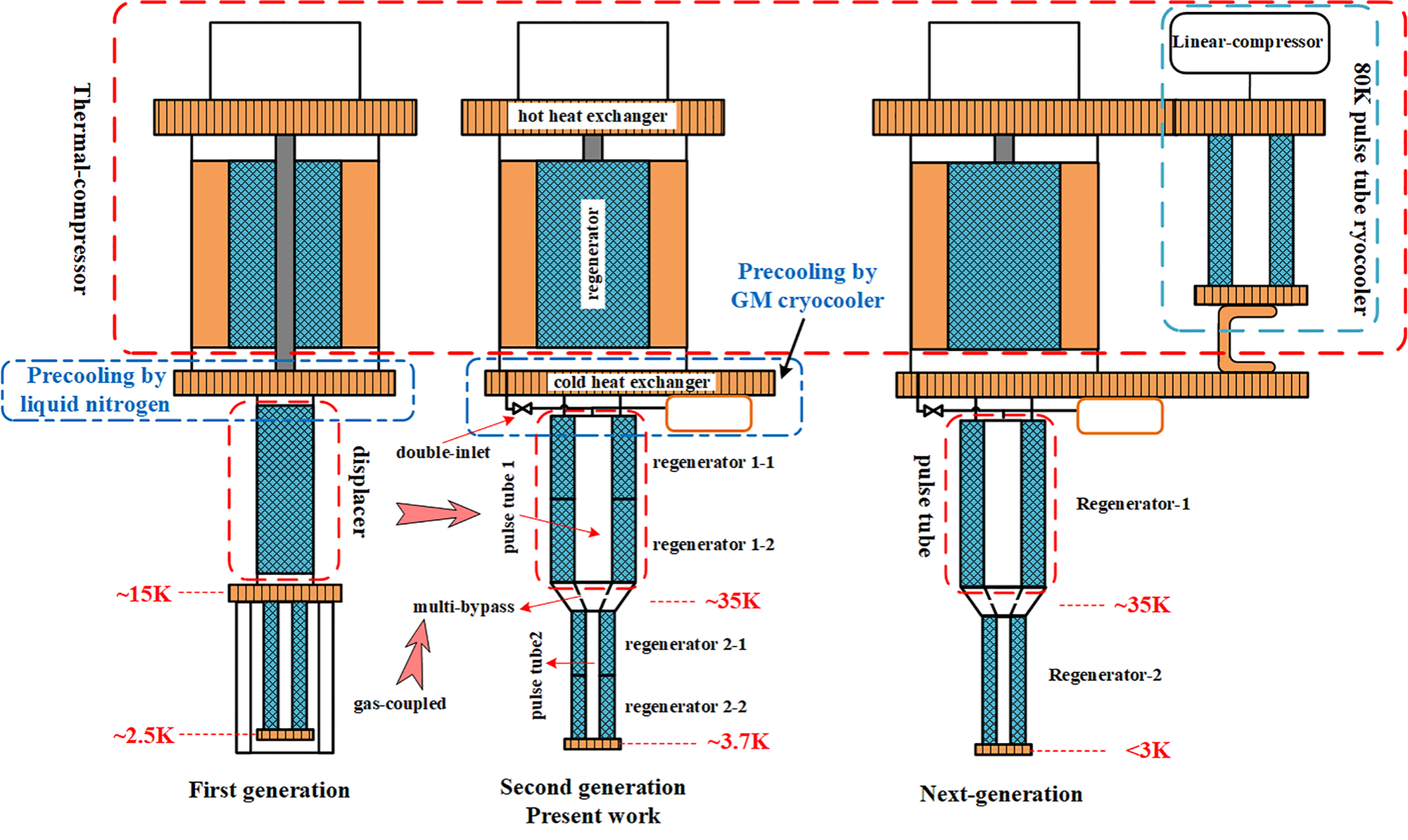
Thermal-compressor
hot heat exchanger
regenerator
Linear-compressor
80K pulse tube ryocooler
Precooling by
GM cryocooler
Precooling by
liquid nitrogen
cold heat exchanger
double-inlet
displacer
pulse tube 1
regenerator 1-1
regenerator 1-2
~15K
multi-bypass
~35K
regenerator 2-1
pulse tube2
gas-coupled
regenerator 2-2
~2.5K
~3.7K
pulse tube
Regenerator-1
~35K
Regenerator-2
<3K
First generation
Second generation
Present work
Next-generation

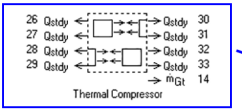

Thermal-compressor

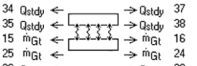

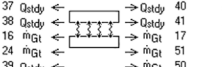

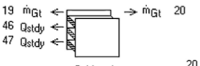

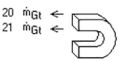

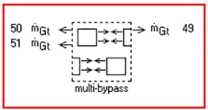

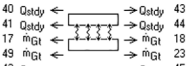

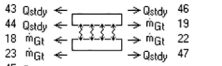

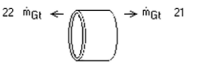

Multi-bypass & Double-inlet

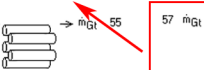

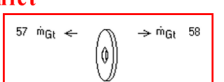

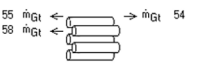

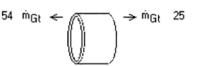

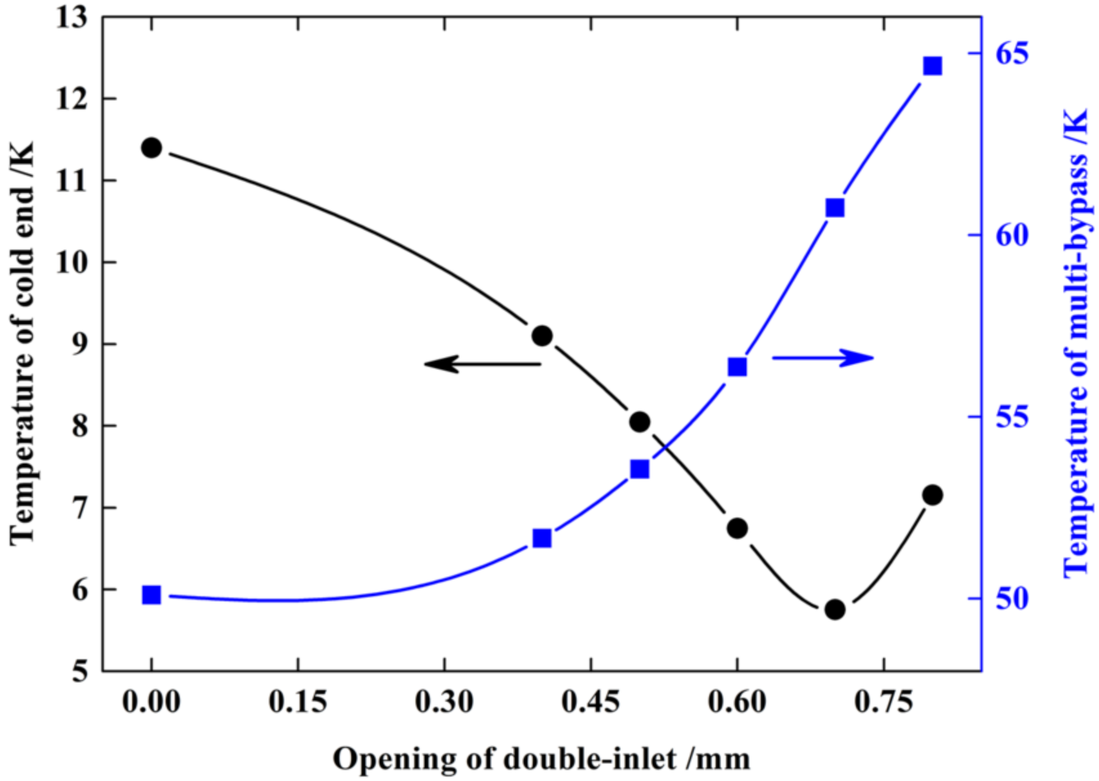
Temperature of cold end /K
Temperature of multi-bypass /K
Opening of double-inlet /mm
13
12
11
10
9
8
7
6
5
65
60
55
50
0.00
0.15
0.30
0.45
0.60
0.75

(a)

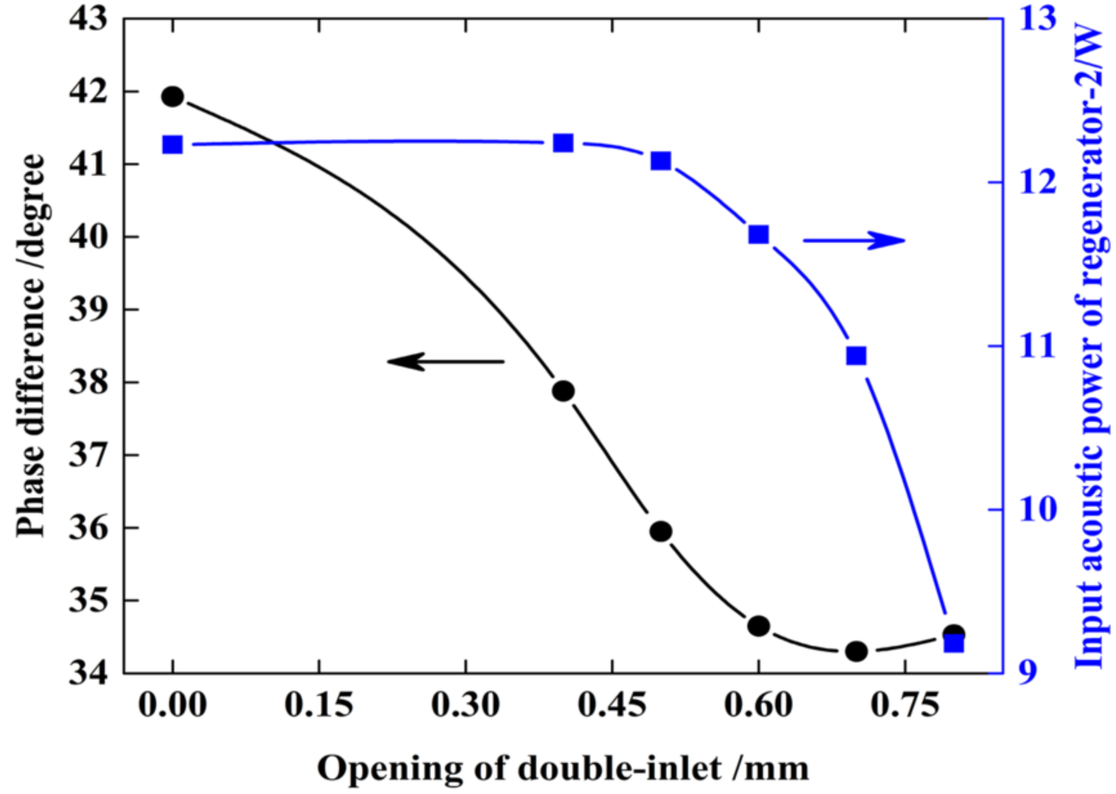
Phase difference /degree
Input acoustic power of regenerator-2/W
Opening of double-inlet /mm
43
42
41
40
39
38
37
36
35
34
13
12
11
10
9
0.00
0.15
0.30
0.45
0.60
0.75

(b)

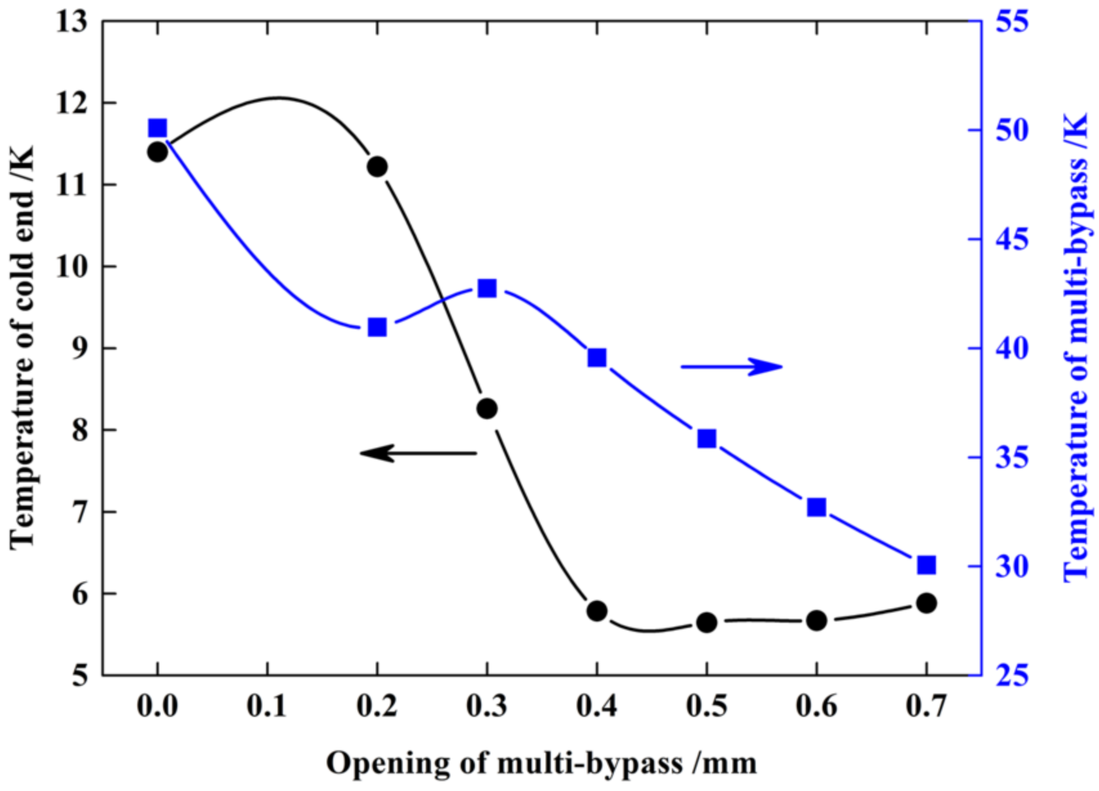
Temperature of cold end /K
Temperature of multi-bypass /K
Opening of multi-bypass /mm
13
12
11
10
9
8
7
6
5
55
50
45
40
35
30
25
0.0
0.1
0.2
0.3
0.4
0.5
0.6
0.7

(c)

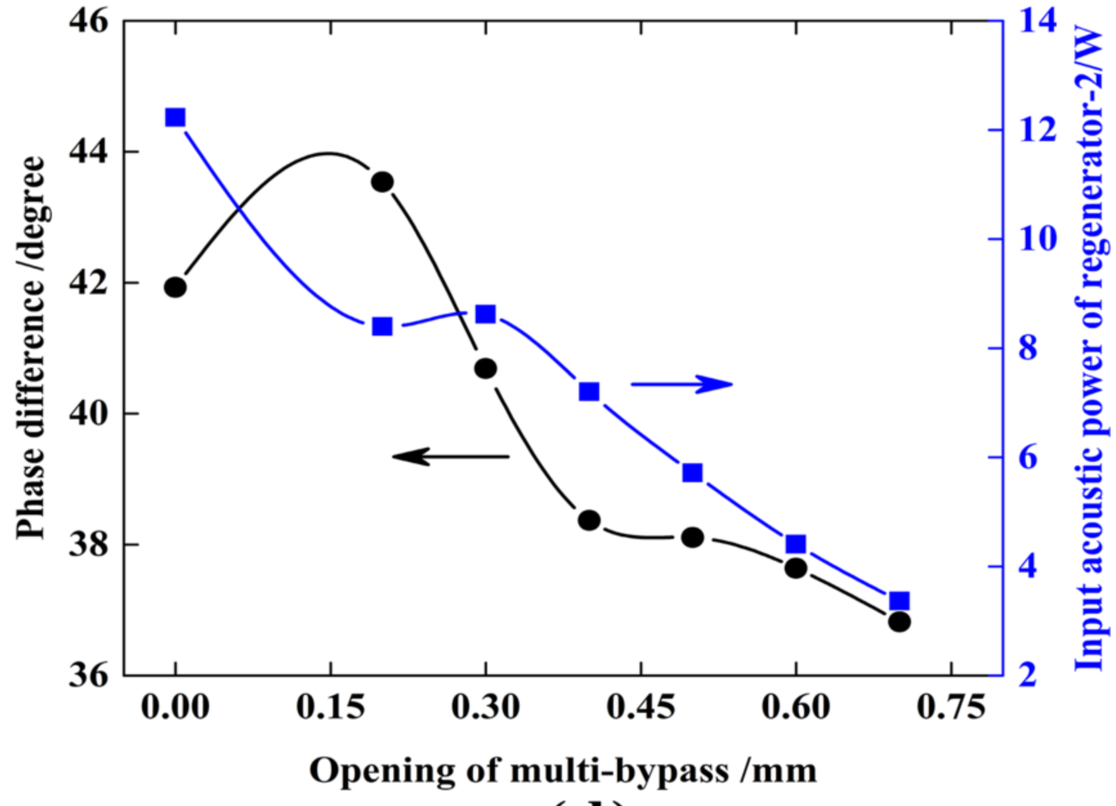
Phase difference /degree
Input acoustic power of regenerator-2/W
Opening of multi-bypass /mm
46
44
42
40
38
36
14
12
10
8
6
4
2
0.00
0.15
0.30
0.45
0.60
0.75

(d)

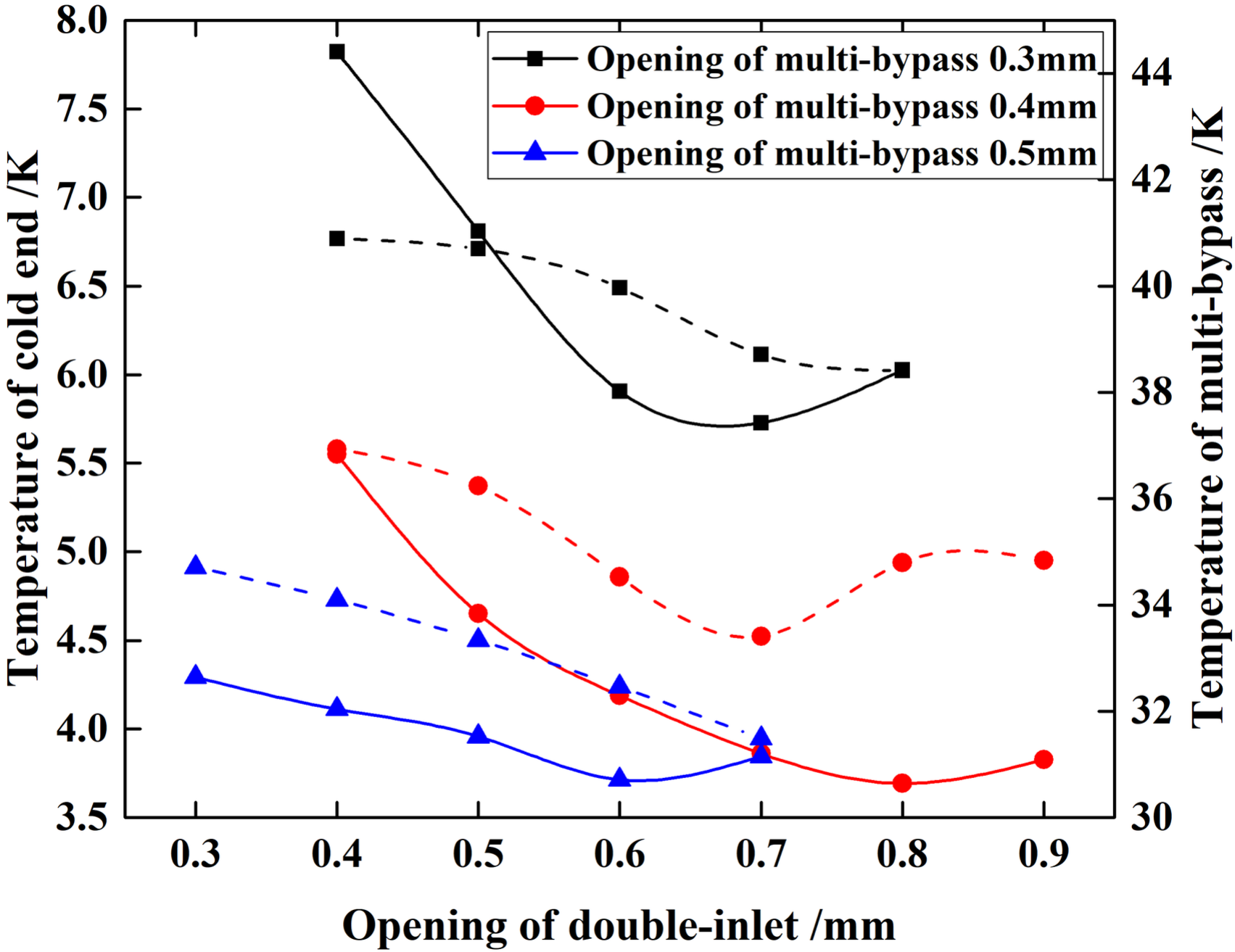
Opening of multi-bypass 0.3mm
Opening of multi-bypass 0.4mm
Opening of multi-bypass 0.5mm
Temperature of cold end /K
Temperature of multi-bypass /K
Opening of double-inlet /mm
8.0
7.5
7.0
6.5
6.0
5.5
5.0
4.5
4.0
3.5
44
42
40
38
36
34
32
30
0.3
0.4
0.5
0.6
0.7
0.8
0.9

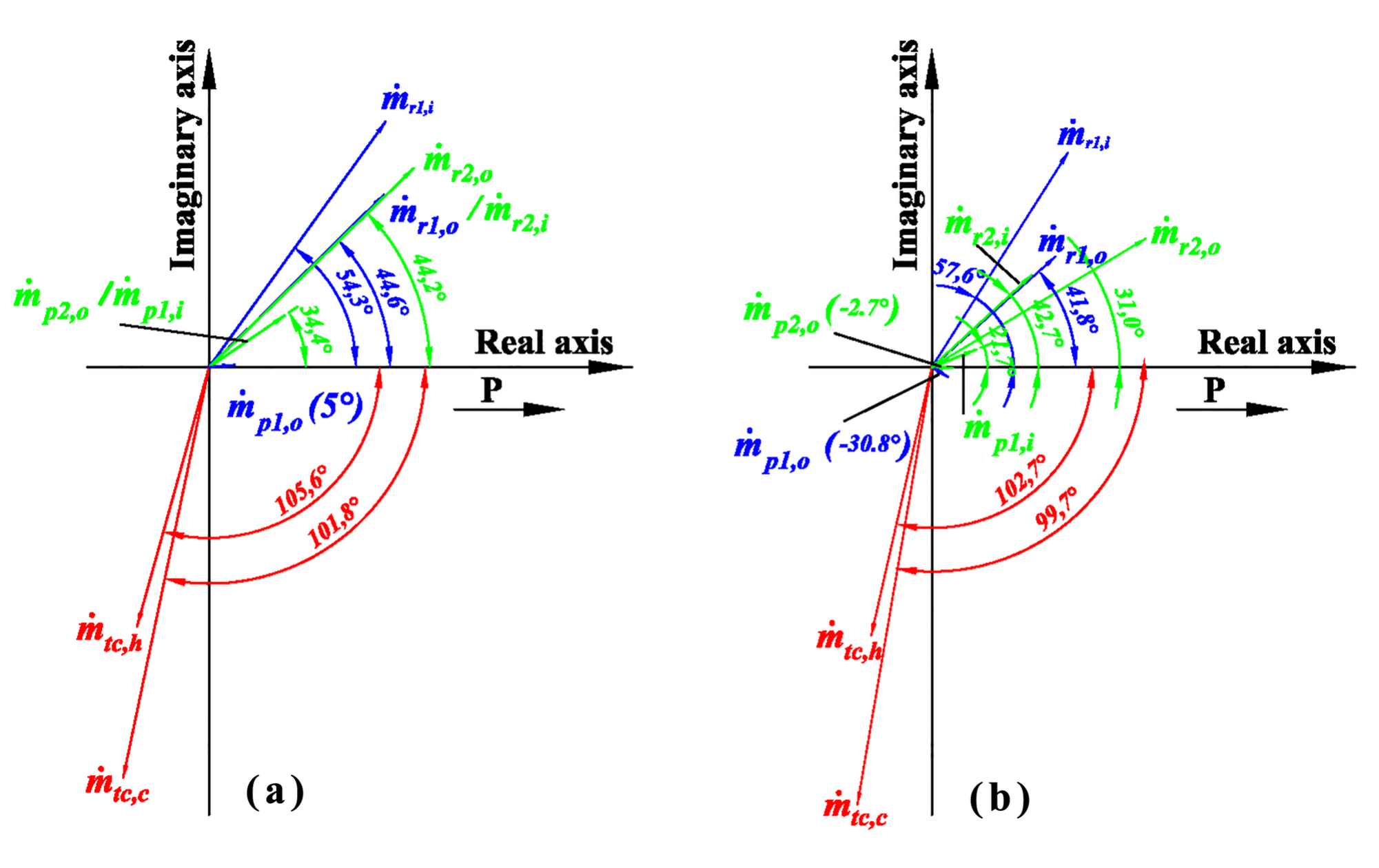
Imaginary axis
Real axis
P
$\dot{m}_{r1,i}$
$\dot{m}_{r2,o}$
$\dot{m}_{r1,o}$ / $\dot{m}_{r2,i}$
$\dot{m}_{p2,o}$ / $\dot{m}_{p1,i}$
$\dot{m}_{p1,o}$ (5°)
54,3°
44,6°
44,2°
34,4°
105,6°
101,8°
$\dot{m}_{tc,h}$
$\dot{m}_{tc,c}$
(a)
Imaginary axis
Real axis
P
$\dot{m}_{r1,i}$
$\dot{m}_{r2,i}$
$\dot{m}_{r1,o}$
$\dot{m}_{r2,o}$
$\dot{m}_{p2,o}$ (-2.7°)
$\dot{m}_{p1,o}$ (-30.8°)
$\dot{m}_{p1,i}$
57,6°
41,8°
42,7°
31,0°
102,7°
99,7°
$\dot{m}_{tc,h}$
$\dot{m}_{tc,c}$
(b)

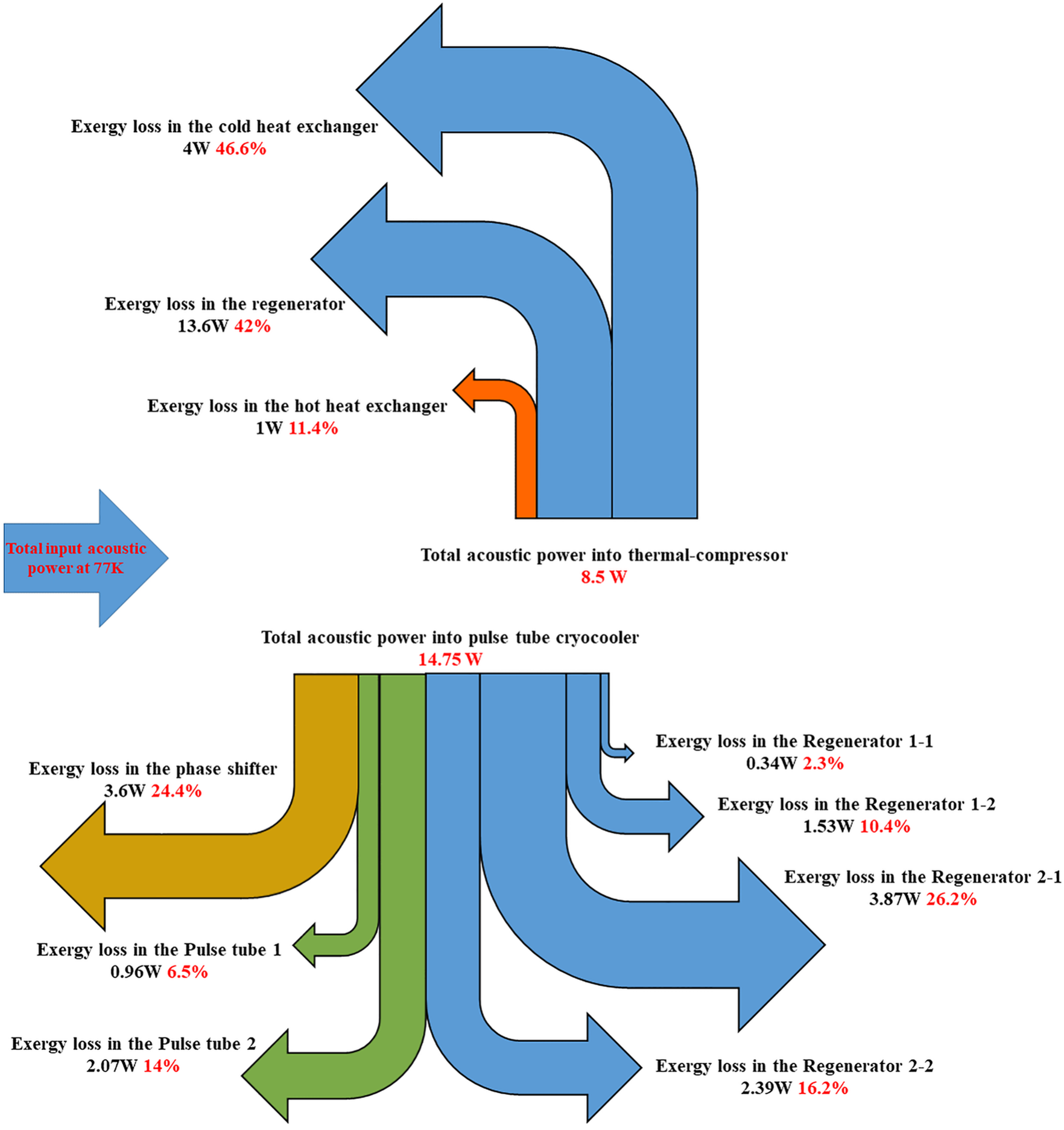
Exergy loss in the cold heat exchanger
4W 46.6%
Exergy loss in the regenerator
13.6W 42%
Exergy loss in the hot heat exchanger
1W 11.4%
Total input acoustic power at 77K
Total acoustic power into thermal-compressor
8.5 W
Total acoustic power into pulse tube cryocooler
14.75 W
Exergy loss in the Regenerator 1-1
0.34W 2.3%
Exergy loss in the Regenerator 1-2
1.53W 10.4%
Exergy loss in the Regenerator 2-1
3.87W 26.2%
Exergy loss in the phase shifter
3.6W 24.4%
Exergy loss in the Pulse tube 1
0.96W 6.5%
Exergy loss in the Pulse tube 2
2.07W 14%
Exergy loss in the Regenerator 2-2
2.39W 16.2%

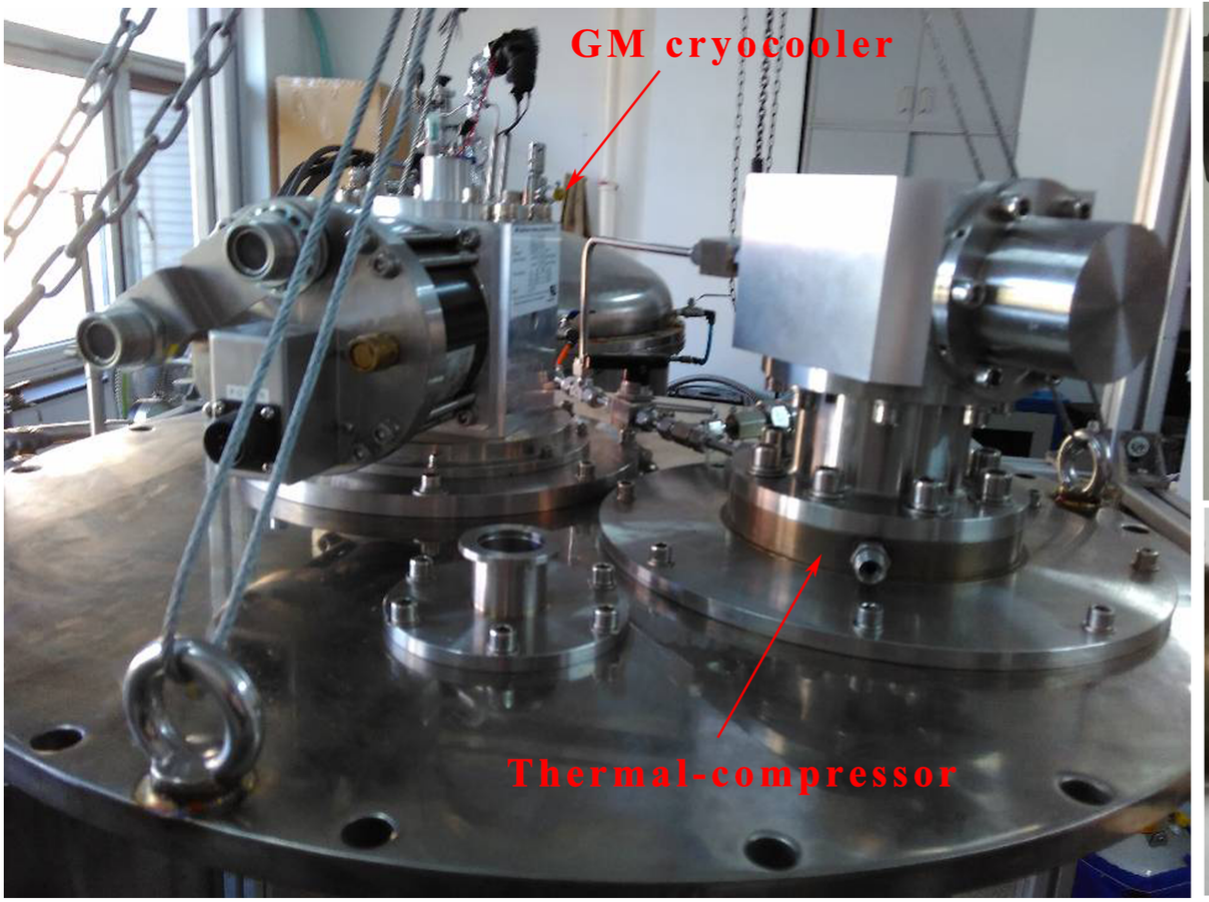
GM cryocooler
Thermal-compressor


pulse tube cryocooler

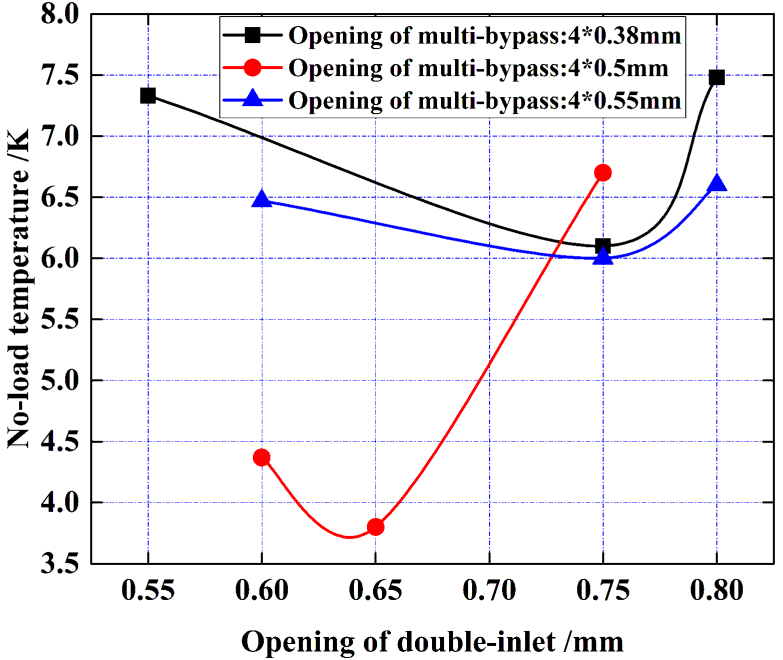
Opening of multi-bypass:4*0.38mm
Opening of multi-bypass:4*0.5mm
Opening of multi-bypass:4*0.55mm
No-load temperature /K
8.0
7.5
7.0
6.5
6.0
5.5
5.0
4.5
4.0
3.5
0.55
0.60
0.65
0.70
0.75
0.80
Opening of double-inlet /mm

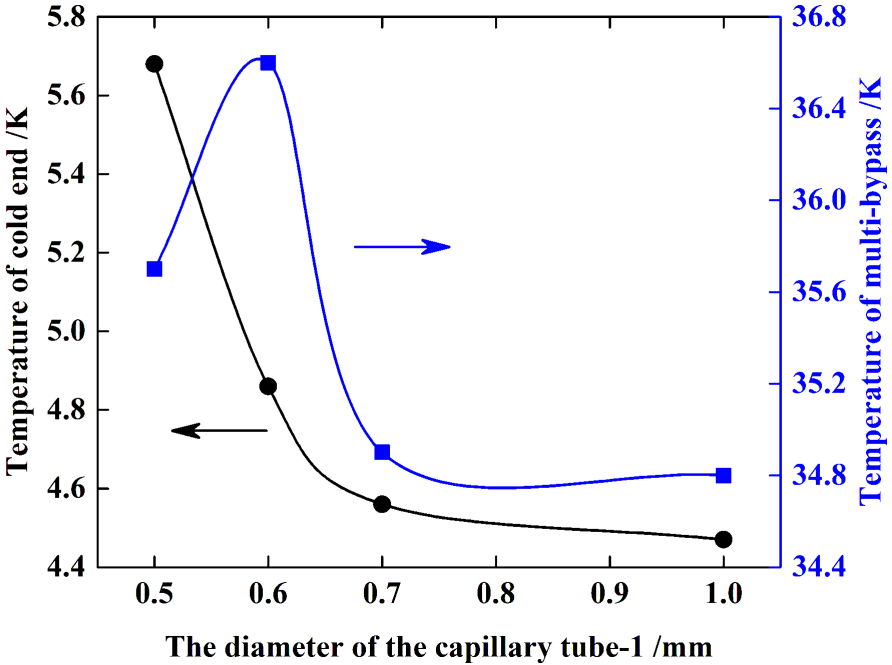
5.8
5.6
5.4
5.2
5.0
4.8
4.6
4.4
Temperature of cold end /K
36.8
36.4
36.0
35.6
35.2
34.8
34.4
Temperature of multi-bypass /K
0.5
0.6
0.7
0.8
0.9
1.0
The diameter of the capillary tube-1 /mm

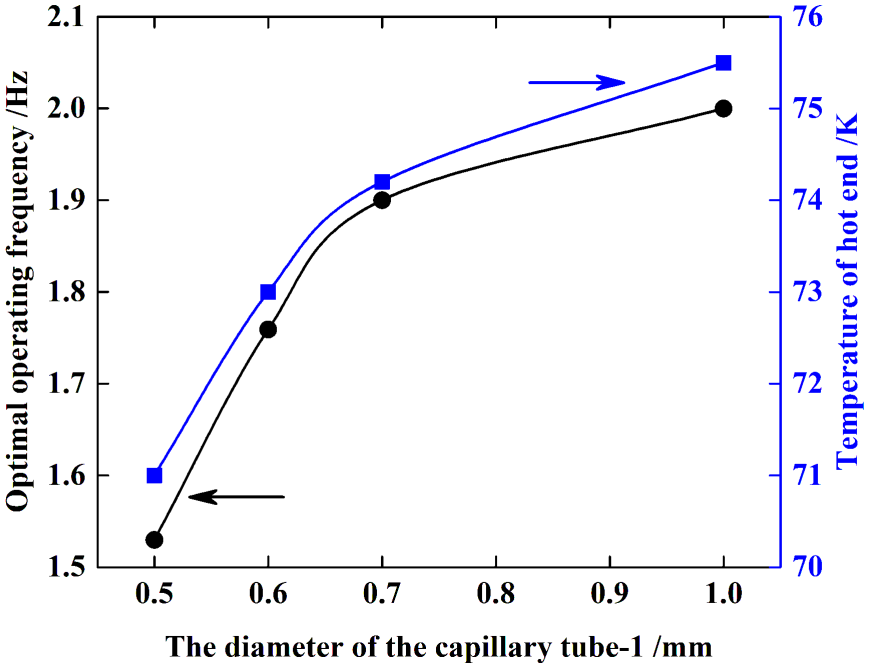
Optimal operating frequency /Hz
Temperature of hot end /K
The diameter of the capillary tube-1 /mm
2.1
2.0
1.9
1.8
1.7
1.6
1.5
76
75
74
73
72
71
70
0.5
0.6
0.7
0.8
0.9
1.0

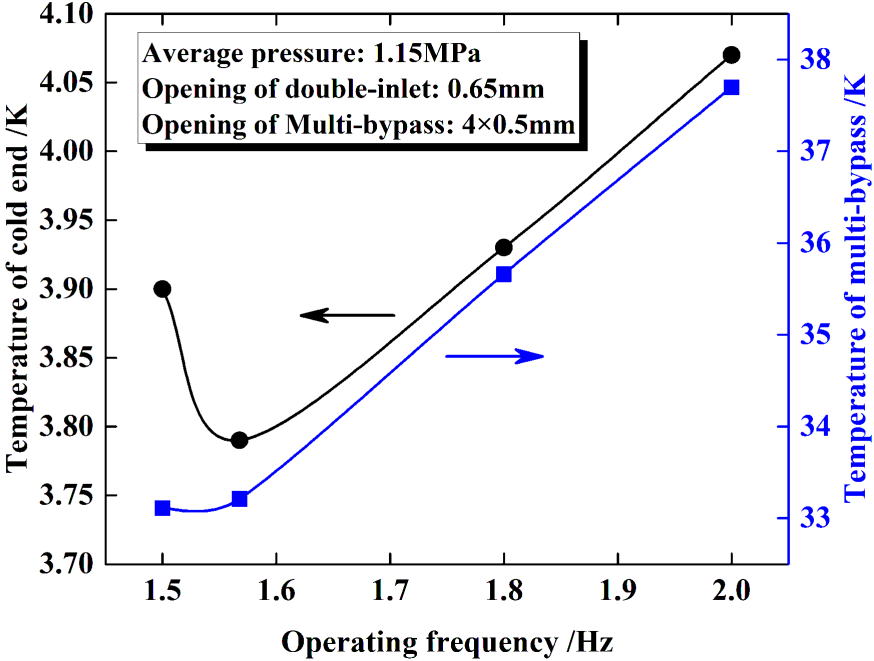
Average pressure: 1.15MPa
Opening of double-inlet: 0.65mm
Opening of Multi-bypass: 4×0.5mm
Temperature of cold end /K
Temperature of multi-bypass /K
Operating frequency /Hz
4.10
4.05
4.00
3.95
3.90
3.85
3.80
3.75
3.70
38
37
36
35
34
33
1.5
1.6
1.7
1.8
1.9
2.0

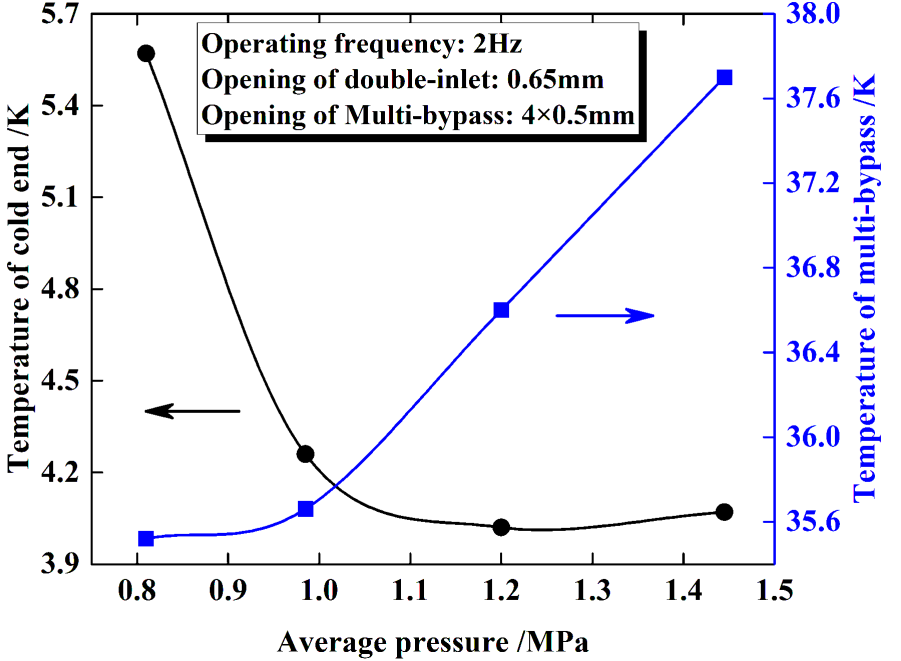
Operating frequency: 2Hz
Opening of double-inlet: 0.65mm
Opening of Multi-bypass: 4×0.5mm
Temperature of cold end /K
Temperature of multi-bypass /K
Average pressure /MPa
5.7
5.4
5.1
4.8
4.5
4.2
3.9
38.0
37.6
37.2
36.8
36.4
36.0
35.6
0.8
0.9
1.0
1.1
1.2
1.3
1.4
1.5

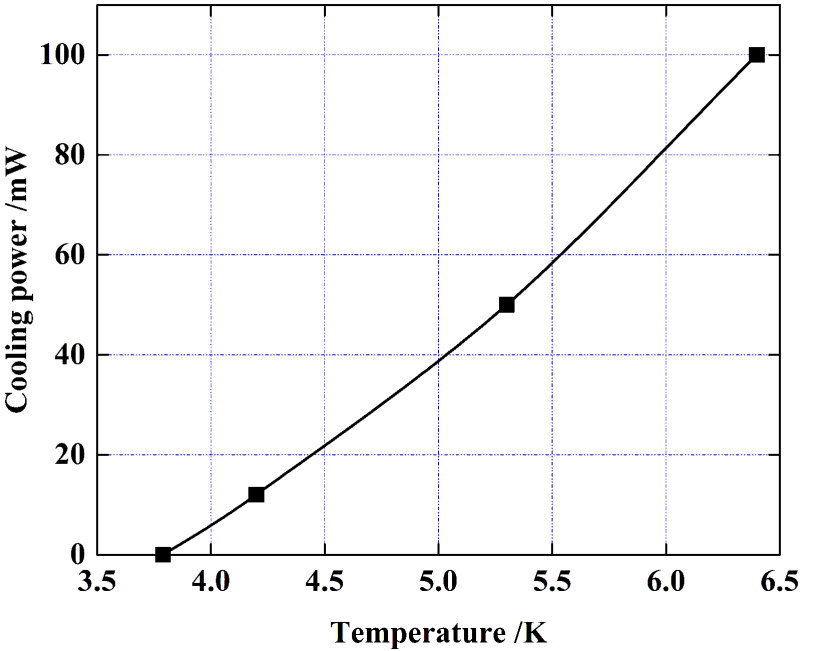
Cooling power /mW
100
80
60
40
20
0
3.5
4.0
4.5
5.0
5.5
6.0
6.5
Temperature /K

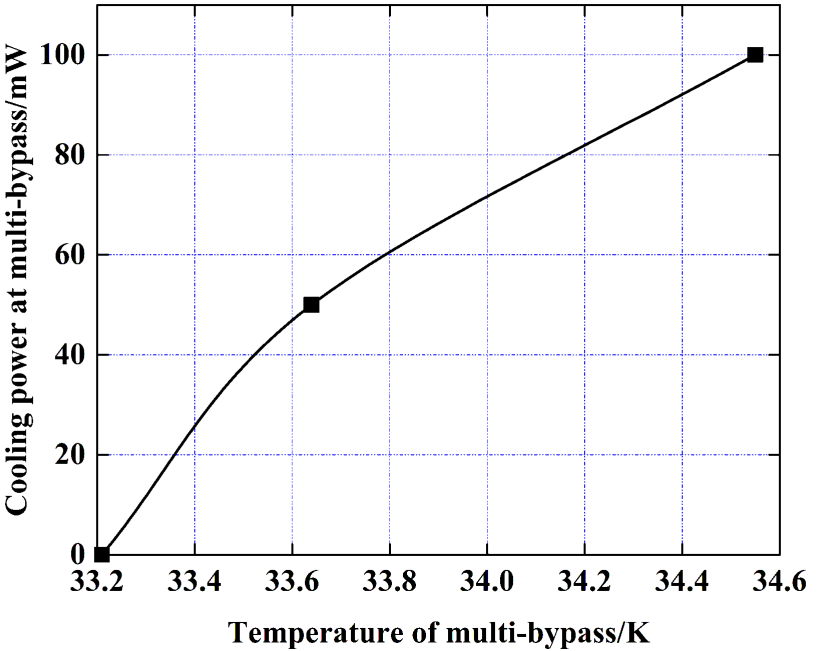
Cooling power at multi-bypass/mW
0
20
40
60
80
100
33.2
33.4
33.6
33.8
34.0
34.2
34.4
34.6
Temperature of multi-bypass/K

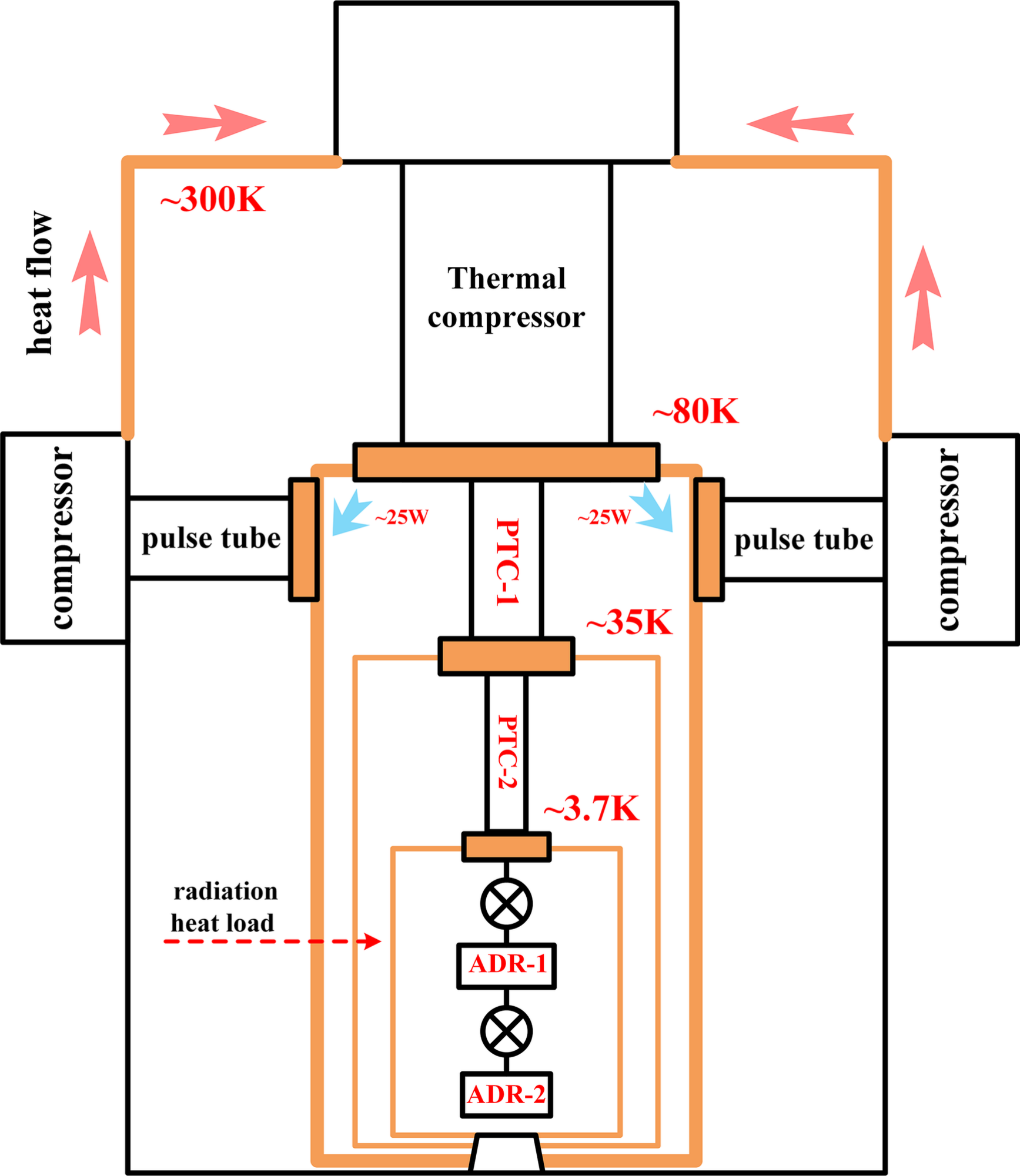
~300K
heat flow
Thermal compressor
~80K
compressor
pulse tube
~25W
PTC-1
~25W
pulse tube
compressor
~35K
PTC-2
~3.7K
radiation heat load
ADR-1
ADR-2